algorithms

MDPI

Article

Application Features of a VOF Method for Simulating Boiling and Condensation Processes

Andrey Kozelkov [1], Andrey Kurkin [1,*], Andrey Puzan [2], Vadim Kurulin [1], Natalya Tarasova [3] and Vitaliy Gerasimov [1]

[1] Department of Applied Mathematics, Nizhny Novgorod State Technical University n.a. R.E. Alekseev, 603155 Nizhny Novgorod, Russia; askozelkov@mail.ru (A.K.); kurulin@mail.ru (V.K.); gervit2008@mail.ru (V.G.)
[2] National Center for Physics and Mathematics, 607328 Sarov, Russia; pppan@yandex.ru
[3] Independent Researcher, 607188 Sarov, Russia; tara271978@mail.ru
* Correspondence: aakurkin@nntu.ru

Abstract

This article presents the results of a study on the possibility of using a single-speed multiphase model with free surface allowance for simulating boiling and condensation processes. The simulation is based on the VOF method, which allows the position of the interphase boundary to be tracked. To increase the stability of the iterative procedure for numerically solving volume fraction transfer equations using a finite volume discretization method on arbitrary unstructured grids, the basic VOF method is been modified by writing these equations in a semi-divergent form. The models of Tanasawa, Lee, and Rohsenow are considered models of interphase mass transfer, in which the evaporated or condensed mass linearly depends on the difference between the local temperature and the saturation temperature with accuracy in empirical parameters. This paper calibrates these empirical parameters for each mass transfer model. The results of our study of the influence of the values of the empirical parameters of models on the intensity of boiling and evaporation, as well as on the dynamics of the interphase boundary, are presented. This research is based on Stefan's problem of the movement of the interphase boundary due to the evaporation of a liquid and the problem of condensation of vapor bubbles water columns. As a result of a series of numerical experiments, it is shown that the average error in the position of the interfacial boundary for the Tanasawa and Lee models does not exceed 3–6%. For the Rohsenow model, the result is somewhat worse, since the interfacial boundary moves faster than it should move according to calculations based on analytical formulas. To investigate the possibility of condensation modeling, the results of a numerical solution of the problem of an emerging condensing vapor bubble are considered. A numerical assessment of its position in space and the shape and dynamics of changes in its diameter over time is carried out using the VOF method, taking into account the free surface. It is shown herein that the Tanasawa model has the highest accuracy for modeling the condensation process using a VOF method taking into account the free surface, while the Rohsenow model is most unstable and prone to deformation of the bubble shape. At the same time, the dynamics of bubble ascent are modeled by all three models. The results obtained confirm the fundamental possibility of using a VOF method to simulate the processes of boiling and condensation and taking into account the dynamics of the free surface. At the same time, the problem of the studied models of phase transitions is revealed, which consists of the need for individual selection of optimal values of empirical parameters for each specific task.

check for updates

Academic Editors: Quanmin Zhu, Jing Chen and Ya Gu

Received: 16 August 2025
Revised: 8 September 2025
Accepted: 16 September 2025
Published: 26 September 2025

Citation: Kozelkov, A.; Kurkin, A.; Puzan, A.; Kurulin, V.; Tarasova, N.; Gerasimov, V. Application Features of a VOF Method for Simulating Boiling and Condensation Processes. *Algorithms* **2025**, *18*, 604. https://doi.org/10.3390/a18100604

Copyright: © 2025 by the authors. Licensee MDPI, Basel, Switzerland. This article is an open access article distributed under the terms and conditions of the Creative Commons Attribution (CC BY) license (https://creativecommons.org/licenses/by/4.0/).

Keywords: fluid dynamics; Navier–Stokes equations; boiling; free surface; mass exchange; vapor; VOF

1. Introduction

Currently, the study of free-surface multiphase flows is of great interest from the point of view of applied and fundamental science [1–5]. Particular attention is paid to the phenomenon of phase change, particularly the processes of boiling, evaporation and condensation. Such processes occur in many engineering systems, such as cooling systems, boilers, heat exchangers, and nuclear reactors. The phase change is characterized by rapid heat transfer due to the high enough speed of this process; therefore, there is a significant effect on the system in general. At the same time, a significant amount of energy is stored in the form of latent heat of vaporization [6]. Therefore, a detailed understanding and a correct description of the phase change process in such systems are important for assessing their reliability and efficient operation. Experimental and detailed studies of the processes of boiling and evaporation are difficult, and therefore the use of numerical simulation is relevant.

In recent decades, several approaches for numerical simulation of free-surface multiphase flows have been presented. In the context of methods for determining the position of the interphase surface, they can be divided into two classes. The first class comprises methods for direct boundary tracing (the Lagrangian approach) [7,8], the basis of which is the fact that the mesh nodes that describe the interface between phases move according to the change in the position of the interface. This approach rearranges the mesh model to accommodate the repositioning of the interphase surface. The second class includes methods for tracking boundaries on a fixed mesh, that is, a Eulerian approach [9,10]. In the Eulerian approach, the geometry of an interphase surface is reconstructed from the value of some marker function that is used to trace that surface. First-class methods provide a high level of accuracy, but they are used for trivial geometric configurations. The methods of the second group are more versatile for computing a wide class of problems involving complex interface deformations, and therefore they are more popular. The Eulerian approach will be used in this work.

Within the framework of the Eulerian approach, several models can be distinguished. The multi-velocity model [11,12] (the so-called Euler–Euler model), in which the equations of motion and continuity are solved separately for each phase, makes it possible to describe the dynamics of a multiphase liquid taking into account the free surface. In this case, each phase has its own velocity and total pressure, and to calculate the volume that each phase occupies in space, volume fraction transfer equations are introduced. The Euler–Euler model is more complex to implement and requires precise closing relations when writing equations [13]. Due to the fact that each of the phases will have its own set of equations solved, the requirements for computing resources will be increased. This model is rarely used, mainly for bubble flow problems [14,15]. The Eulerian approach using the volume fraction of a liquid as a marker function, called the VOF (volume of fluid) method, has several practical applications [9,16,17]. This method is a simplified one-speed Euler–Euler model, where one set of equations of motion and continuity are solved for all phases, and the volume fraction transfer equation is solved for each phase. This model allows flows with a free surface—including stratified flows, liquid splashing, filling or emptying tanks, movement of gas bubbles in a liquid [18], and crushing of liquid jets due to surface tension—to be described [18,19]. This model is less demanding in terms of computational resources than the Euler–Euler model and can be adapted to perform calculations on arbitrary

unstructured grids. A review of the relevant literature on multiphase computational fluid dynamics methods shows that the one-speed VOF method is the most convenient to implement and promising to use, since it allows us to consider the simulated liquid–gas system as a single one-speed medium with variable physical properties. The key advantage of this method is its adaptability to the application of finite volume sampling on cells of an arbitrary shape [3,16,17].

The key issue when applying the VOF method to the simulation of phase transitions, namely for boiling and condensation, is the computation of the mass that undergoes phase transformation. Thus, in the classical theories of Herz-Knudsen [20] and Schrage [21], semi-empirical relations are used to calculate the interphase mass flow. Empirical parameters in such models are mainly selected by comparing the calculated mass flow with experimental data and then adjusting these parameters to reduce the relative error, which limits the applicability of these models to arbitrary cases. A variety of models of this type are presented in [22]. Some of the most widely used models in engineering computations are the Tanasawa model [23], Lee model [24], and Rohsenow model [25]. In all these models, an empirical coefficient is used to connect the mass flow across the liquid–vapor interface with the temperature, which requires matching in accordance with the conditions of the problem. In this case, the values of the coefficients and the form of dependence for these models are different from each other. One should take into account that for each specific experimental case of the phase transition, it is necessary to empirically match the indicated coefficients. This is due to several key points: heat transfer surfaces have different physical properties (roughness, thermal conductivity, wettability); heat transfer can occur in different conditions (temperature levels, heater power); and working fluid properties can vary significantly (saturation temperature, thermal conductivity coefficient, heat capacity).

Thus, the Tanasawa model is a simplified Schrage model, where the temperature at the interface is equal to the saturation temperature. The heat flow on the free surface is linearly dependent on the temperature difference between the liquid and the vapor at a given point. The Lee model is based on the assumption that the mass transition occurs at constant pressure and quasi-thermal equilibrium. In the Tanasawa model, it is assumed that the temperature of the liquid is equal to the temperature of the vapor–liquid mixture, and the entire heat flow through the interface goes to mass exchange.

These models are used in the modeling of phase transitions based on the VOF method. The Tanasawa model [23] can be found in [26–28], where the model is used to calculate the dynamics of the ascent of a single bubble and the dynamics of the boiling flow. The value of the empirical parameter of the model is either not specified or is taken from preliminary test calculations.

The Lee model [24] was used in [29], in which the characteristics of the refrigerant flow were numerically investigated based on the Fluent program code, taking into account the boiling process. It is assumed that at the studied values of pressure and temperature, the liquid refrigerant boils intensively in local areas of the pipeline. The value of the empirical parameter of the Lee model, equal to 100, was used. Pressure graphs in the extinguishing agent tank were obtained, but the effect of an empirical parameter on the amount of vaporized liquid was not studied, and this may have affected the pressure distribution. In [30], the Fluent code with the Lee model was also used to calculate the mass transfer during boiling of flow in microchannels. In this work, the boiling mode was bubbly, and the authors used the standard value of the empirical parameter of the boiling model (i.e., equal to 0.1).

In [31], a hybrid Lee and Tanasawa model implemented in OpenFOAM computational code is proposed to simulate a two-phase flow in a thermosiphon. In this task, there

is an evaporator and a condenser, and the evaporation and condensation processes are continuous and simultaneous. Therefore, the correct choice of an empirical parameter is important for minimizing the modeling error. The paper indicates that the values of empirical parameters 10^4 and 10^{-2} are used for the Lee and Tanasawa models, respectively, but how they are selected is not specified.

The Rohsenow model [25] is used in [32] to model boiling flows, while the values of the empirical parameter of the model are not specified.

As the review showed, when studying multiphase flows taking into account boiling and condensation, the authors often use some value of the empirical parameter of phase transition models, without investigating the effect of its value on the calculation results. In this paper, a similar study is conducted for finite volume discretization of equations on arbitrary unstructured grids, and recommendations are given regarding the choice of models of phase transitions and values of empirical models, respectively.

In this paper, we consider a mathematical model of a VOF method, supplemented by models of phase transitions from Tanasawa, Lee, and Rohsenow. The continuous force surface model (CFS) proposed in [33] is used to account for the surface tension force in the momentum conservation equation. A modification of the mathematical model is presented, which provides an increase in the stability of the iterative numerical solution procedure for finite volume discretization of equations on arbitrary unstructured grids. Numerical simulations of boiling and condensation are carried out on two problems with analytical or experimental data: the Stefan problem on the movement of the interphase boundary due to liquid evaporation [34], and the problem of condensation of a vapor bubble in a water column [35]. The results are obtained for three models of phase transitions (Tanasawa, Lee, and Rohsenow) with varying empirical parameters within the models. The problem of the phase transition models under consideration is shown: the optimal value of empirical parameters should be selected for each task and formulation, depending on the conditions of the task, the parameters of the computational model, and the characteristic size of the grid model cells.

2. Physical and Mathematical Model

The motion of a multiphase medium with a free surface in the approximation, taking into account phase change using the VOF method for tracking the interface between phases, is described using a system of Navier–Stokes equations for the entire medium, which are supplemented by the transfer equations of the volume fraction of each phase [3,36]:

$$\begin{cases} \dfrac{\partial \rho}{\partial t} + \nabla \cdot (\rho \vec{u}) = \sum\limits_k S_{\alpha_k}, \\ \dfrac{\partial \rho \vec{u}}{\partial t} + \nabla \cdot (\rho \vec{u} \vec{u}) = -\nabla p + \nabla \cdot \left[\mu \left(\nabla \vec{u} + \nabla \vec{u}^T \right) \right] + \rho \vec{g} + \vec{F}_{st}, \\ \dfrac{\partial \rho_k \alpha_k}{\partial t} + \nabla \cdot \left(\rho_k \alpha_k \vec{u} \right) = S_{\alpha_k}, \\ \dfrac{\partial \rho C_p T}{\partial t} + \nabla \cdot (\rho C_p T \vec{u}) = \nabla \cdot (\lambda \nabla T) + S_E. \end{cases} \quad (1)$$

Here, ρ, $\vec{u}$, T, p are the density, velocity, temperature and pressure of the medium, respectively; μ, λ, C_p are the viscosity, thermal conductivity coefficient, and heat capacity of multiphase medium; S_E is the energy source term; $\vec{g}$ is the gravity acceleration vector; t is time; $\alpha_k = V_k/V$ are the volume fractions of the k-th phase; and ρ_k is the density of the

k-th phase. The general physical parameters of the multiphase medium are related to the parameters of the individual phases as follows:

$$\rho = \sum_{k=1}^{N} \rho_k \alpha_k,\ \mu = \sum_{k=1}^{N} \mu_k \alpha_k,\ C_p = \sum_{k=1}^{N} \frac{C_{p,k}\rho_k}{\rho}\ \alpha_k,\ \lambda = \sum_{k=1}^{N} \lambda_k \alpha_k.$$

When simulating boiling, two phases are considered: index l is a liquid phase, and index ν is vapor. If we presume the phases incompressible and the source to be $S_{\alpha_l} = -S_{\alpha_\nu} \equiv \dot{m}$, the system of Equation (1) can be written as follows:

$$\begin{cases} \nabla \cdot \vec{u} = \dot{m}\left(\frac{1}{\rho_l} - \frac{1}{\rho_\nu}\right), \\ \frac{\partial \rho \vec{u}}{\partial t} + \nabla \cdot (\rho \vec{u}\vec{u}) = -\nabla p + \nabla \cdot \left[\mu\left(\nabla \vec{u} + \nabla \vec{u}^T\right)\right] + \rho \vec{g} + \vec{F}_{st}, \\ \frac{\partial \rho C_p T}{\partial t} + \nabla \cdot (\rho C_p T \vec{u}) = \nabla \cdot (\lambda \nabla T) + \dot{m} h_{\nu l}, \\ \frac{\partial \alpha_l}{\partial t} + \nabla \cdot \left(\alpha_l \vec{u}\right) = \frac{\dot{m}}{\rho_l}, \\ \frac{\partial \alpha_\nu}{\partial t} + \nabla \cdot \left(\alpha_\nu \vec{u}\right) = -\frac{\dot{m}}{\rho_\nu}. \end{cases} \tag{2}$$

Here, $h_{\nu l}$ is latent heat of vaporization.

When there is a phase interface in homogeneous equations of motion, volumetric power sources appear, and they are associated with the surface tension forces $\vec{F}_{st}$. The continuous surface force (CSF) model proposed in [33] is used to account for the surface tension force in the momentum conservation equation. Within this model, the normal component of the force is considered, and the tangential component is neglected. The surface tension factor along the interface does not change. In this approximation, the surface tension effect is represented as a continuous volumetric force acting at the interface in the transition region:

$$\vec{F}_{st} \approx \sigma \mathrm{k} \nabla \alpha_i.$$

Here, σ is the surface tension, $\mathrm{k} = -\nabla \cdot \left(\frac{\nabla \alpha_i}{|\nabla \alpha_i|}\right)$ is the interfacial curvature.

When computing the curvature from the exact values of the volume fraction, due to the field discontinuity of this value and the actual calculation of the second derivative of this discontinuous field, calculation errors occur that lead to an increase in "parasitic" oscillations in the velocity field with time. Such oscillations, in their turn, can lead to instability in the solution and destruction of the interface. To improve stability and reduce oscillations, a smoothing procedure is used before computing the curvature. Therefore, the curvature is calculated from the smoothed volume fraction:

$$\mathrm{k} = -\nabla \cdot \left(\frac{\nabla \widetilde{\alpha}_i}{|\nabla \widetilde{\alpha}_i|}\right).$$

Here, $\widetilde{\alpha}$ is the smoothed volume fraction.

Different methods can be used for smoothing. We use the following type of smoothing in this work [37]:

$$\widetilde{\alpha}_{i,P} = \frac{\sum\limits_{f=1}^{N} \alpha_{i,f} S_f}{\sum\limits_{f=1}^{N} S_f}.$$

Here, S_f is the area of the face of the cell P, and $\alpha_{i,f}$ is the value of the volume fraction interpolated in the center of the face.

Several models of interfacial mass transfer as a result of boiling and condensation processes are considered in this work.

The Tanasawa model proposed in [23] is considered first. Kinetic theory is used to relate the intensity of the interphase mass transfer to the deviation of the local temperature from the saturation temperature. Using kinetic approximation, the volumetric mass flow $\dot{m}(\frac{kg}{m^3 \cdot s})$ can be calculated in the interface area as follows:

$$\dot{m} = \varphi(T - T_{sat})|\nabla \alpha_l|, \ \varphi = \frac{2\gamma}{2-\gamma}\left(\frac{M}{2\pi R_g}\right)^{1/2}\frac{\rho_v h_{vl}}{T_{sat}^{3/2}}, \tag{3}$$

where h_{lv} is the latent heat of evaporation, γ is the condensing coefficient/evaporation coefficient (or accommodation coefficient), M is the molar weight, R_g is the universal gas constant, and T_{sat} is the saturation temperature at a given pressure.

In this approach, the interface surface area for each mixed cell is assumed to be $S_{int} = |\nabla \alpha_l| \cdot V_{cell}$, and $\dot{m} \neq 0$ only in the region of the interface, where there is a change in phase volume fractions. The value $\dot{m}$ is positive for evaporation ($T > T_{sat}$) and negative for condensation ($T < T_{sat}$).

The study in [23] provides examples of the experimentally calculated accommodation coefficient γ from different sources. It should be noted that the range of variation of the coefficient is quite large, from small values of 0.006 to values of 1. At the same time, small values prevail in the experiments for single air bubbles suspended in water.

Another model widely used for simplicity is the Lee model [24]. It is assumed that phase change occurs at constant pressure in a state of thermal quasi-equilibrium and corresponds to the following expressions:

$$\begin{cases} \dot{m} = r\alpha_l \rho_l \frac{T - T_{sat}}{T_{sat}} \text{ for } T > T_{sat}, \\ \dot{m} = r\alpha_v \rho_v \frac{T - T_{sat}}{T_{sat}} \text{ for } T < T_{sat}. \end{cases} \tag{4}$$

An empirical coefficient called the mass transfer intensity coefficient (which comprises the specific interphase surface area) also has a large range of values depending on flow geometry, mesh resolution, time step, and environmental conditions [38]. Some researchers determine a value of 0.1, and others use a value of 100. It has been found that the higher the value of this coefficient, the less the interface temperature differs from the saturation temperature. Despite the fact that some researchers point out possible problems of numerical convergence at too high values, r values of about 7.5×10^5~1.0×10^7 1/s are often used at more intensive mass exchange.

This paper also considers the source of mass used in the Rohsenow model [25]:

$$\dot{m} = \frac{Qs \times (T - T_{sat})}{h_{vl}}, \tag{5}$$

where Qs is the heat transfer coefficient between the vapor bubbles and the surrounding liquid multiplied by the interphase contact surface area reduced per unit volume. This model is applicable for volumetric boiling with the formation of vapor bubbles, while it is assumed that all bubbles are at the saturation temperature, the temperature of the liquid is equal to the temperature of the vapor–liquid mixture, and the entire heat flow through the interface goes to mass exchange. In open works, no recommendations have been found on what Qs values should be used for solving applied problems.

3. Increasing the Stability of the Numerical Solution

To stabilize the iterative numerical solution procedure when discretizing the transfer equations of the volume fractions, these equations are written in semi-divergent form [39]:

$$\frac{\partial \alpha_l}{\partial t} + \nabla \cdot \left(\alpha_l \vec{u}\right) - \alpha_l \nabla \cdot \vec{u} = \frac{\dot{m}}{\rho_l} - \alpha_l \dot{m}\left(\frac{1}{\rho_l} - \frac{1}{\rho_v}\right).$$

This compensates for approximation errors associated with inaccurate fulfillment of the volumetric flow balance condition for the cell. In this case, when calculating the convective term, total equality of inflowing and outflowing fluxes is imposed.

In order to improve the stability of the computation and reduce the imbalance introduced into the numerical scheme by the gap in the fields of physical parameters when crossing the interface, it is necessary to use a volumetric flow instead of a mass flow during discretization. Moreover, due to the gap in the heat capacity field, it is advisable to write the energy conservation equation with regard to enthalpy [40].

In this case, system of Equation (2) is written as follows:

$$\begin{cases} \operatorname{div} \vec{u} = \left(\frac{1}{\rho_l} - \frac{1}{\rho_v}\right)\dot{m}, \\ \frac{\partial \rho \vec{u}}{\partial t} + \nabla \cdot (\rho \vec{u}\vec{u}) = -\nabla p + \nabla \cdot \left[\mu\left(\nabla \vec{u} + \nabla \vec{u}^T\right)\right] + \rho \vec{g} + \vec{F}_{st}, \\ \frac{\partial h}{\partial t} + \vec{u} \cdot \nabla h = \frac{1}{\rho}\nabla \cdot \left(\lambda \nabla \frac{h}{\rho}\right) + \frac{1}{\rho}\dot{m}h_{vl}, \\ \frac{\partial \alpha_l}{\partial t} + \nabla \cdot \left(\alpha_l \vec{u}\right) - \alpha_l \nabla \cdot \vec{u} = \frac{\dot{m}}{\rho_l} - \alpha_l \dot{m}\left(\frac{1}{\rho_l} - \frac{1}{\rho_v}\right), \\ \frac{\partial \alpha_v}{\partial t} + \nabla \cdot \left(\alpha_v \vec{u}\right) - \alpha_v \nabla \cdot \vec{u} = \frac{\dot{m}}{\rho_v} - \alpha_v \dot{m}\left(\frac{1}{\rho_l} - \frac{1}{\rho_v}\right). \end{cases} \quad (6)$$

To enhance the diagonal predominance in the SLAE (System of Linear Algebraic Equations) when discretizing the energy conservation equation, the source term is decomposed into a Taylor series relative to the enthalpy in the vicinity of the point h^n. Taking the first two terms of the decomposition, we obtain:

$$\dot{m}(h) = \dot{m}(h^n) + \frac{\partial \dot{m}}{\partial T}\frac{1}{c_p}(h^{n+1} - h^n).$$

In the case of the Tanasawa model, the source in the energy equation is

$$\dot{m}(h) = \varphi(T^n - T_{sat})|\nabla \alpha_l| + \varphi|\nabla \alpha_l|\frac{1}{c_p}(h^{n+1} - h^n), \quad (7)$$

In the case of the Lee model,

$$\begin{cases} \dot{m}(h) = r\alpha_l\rho_l\frac{T^n - T_{sat}}{T_{sat}} + \frac{r\alpha_l\rho_l}{T_{sat}}\frac{1}{c_p}(h^{n+1} - h^n) \text{ for } T > T_{sat}, \\ \dot{m}(h) = r\alpha_v\rho_v\frac{T^n - T_{sat}}{T_{sat}} + \frac{r\alpha_v\rho_v}{T_{sat}}\frac{1}{c_p}(h^{n+1} - h^n) \text{ for } T < T_{sat}. \end{cases}, \quad (8)$$

And in the case of the Rohsenow model,

$$\dot{m}(h) = \frac{Qs \cdot (T^n - T_{sat})}{h_{vl}} + \frac{Qs}{h_{vl}}\frac{1}{c_p}(h^{n+1} - h^n). \quad (9)$$

Thus, the system of Equation (6) together with models (7)–(9) makes it possible to describe the process of movement of a multiphase medium with a free surface in a single-speed approximation, taking into account phase change. For the numerical solution of this system, we use the SIMPLE method based on the principle of splitting by physical variables and the field correction procedure [41].

The described methods and models are implemented in the Russian LOGOS software package version 5.3.24 [4,42] designed to simulate the conjugate three-dimensional problems of convective heat and mass transfer, aerodynamics, and strength on highly parallel computers. Discretization of the system of Equation (6) is based on the finite volume method on unstructured meshes [3,36]. Acceleration of computations with high-performance supercomputers is carried out using a multi-mesh method [41].

4. Results of Numerical Computations

4.1. The Stefan Problem

A classic problem for the verification of boiling and evaporation models is the Stefan problem, which deals with the motion of a flat interface between steam and liquid determined by vaporization of the liquid due to interaction with superheated steam. The problem has an analytical solution for the speed of interface movement [34]. Initially, there is a liquid and a vapor layer; they are considered incompressible and stationary and in equilibrium. The temperature of the vapor and liquid at the initial moment of time is equal to the saturation temperature; then, the temperature of the steam increases due to the heat coming from the heated wall at a temperature higher than the saturation temperature. The vapor displaces the liquid as it evaporates, which allows the interface to move between them in the direction of the heated wall. The problem is schematically shown in Figure 1.

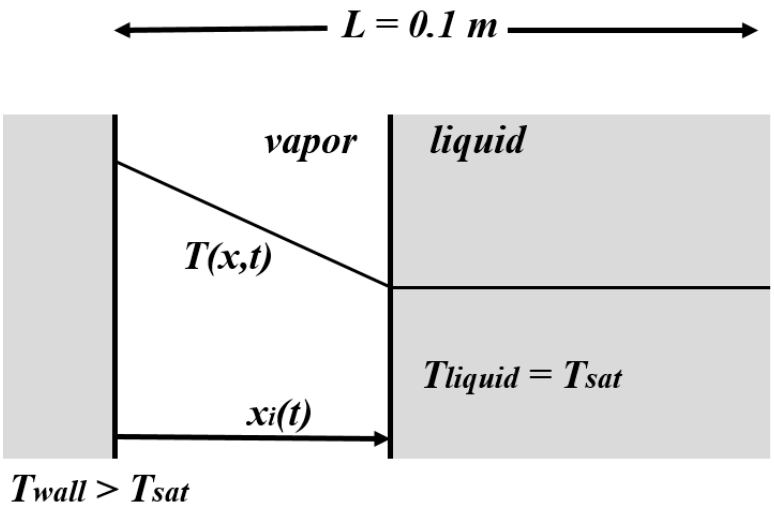


Figure 1. Layout of the Stefan problem.

According to [34], the analytical dependence of the interface position on time and temperature distribution can be found from the following.

$$x_i(t) = 2\zeta\sqrt{D_v t} \text{ is position of the interface, and}$$

$$T(x,t) = T_w - \frac{(T_w - T_{sat})}{erf(\zeta)} erf\left(\frac{x}{2\sqrt{D_v t}}\right) \text{ is the temperature distribution.}$$

Here, $D_v = \frac{k_v}{\rho_v c_v}$ is the thermal diffusivity of the vapor, and constant ζ is calculated from the solution of the following equation.

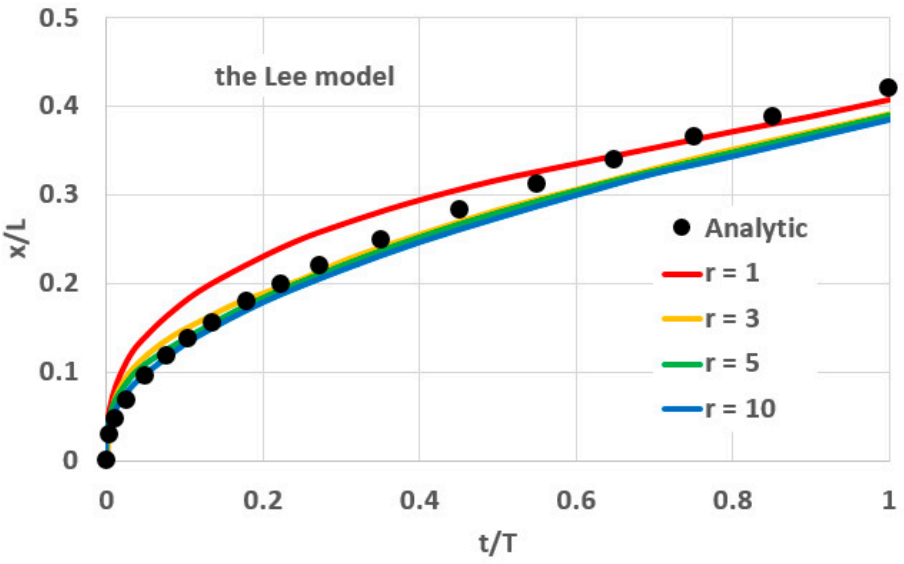
$$\zeta \exp(\zeta^2) erf(\zeta) = \frac{c_v(T_w - T_{sat})}{\sqrt{\pi} h_{vl}}, \; erf(\,) \text{ is an error function.} \quad (10)$$

A region of length $L = 0.1$ m is selected for numerical solution, where a one-dimensional computation mesh is generated with a cell size of $\Delta x = 10^{-3}$ L. The left boundary is an impermeable wall with the temperature $T_w (T_w - T_{sat} = 25$ K), and the right boundary is a boundary with fixed pressure. At the initial time point, vapor occupies two cells adjacent to the heated wall. The numerical simulation is performed for three variants of water saturation pressure, for which there are analytical solutions in [34]—(a) 101.3 kPa, (b) 571 kPa, (c) 14.044 MPa—until the time point $T = 2000$ s. Table 1 shows the respective parameters of the materials.

Table 1. Parameters of the materials.

	Vapor (v)			**Liquid (*l*)**		
	(a)	**(b)**	**(c)**	**(a)**	**(b)**	**(c)**
Boiling temperature (saturation temperature), K (T_{sat})	–	–	–	373	428	609
Density, kg/m^3 (ρ)	0.59	2.92	87	958	912	640
Dynamic viscosity, Pa · s (μ)	1.2×10^{-5}	1.4×10^{-5}	2.4×10^{-5}	2.8×10^{-4}	1.8×10^{-4}	8.1×10^{-5}
Thermal conductivity, W/(m·K) (k)	2.3×10^{-2}	2.8×10^{-2}	8.7×10^{-2}	68.3×10^{-2}	68.4×10^{-2}	46.5×10^{-2}
Specific heat capacity, J/(kg·K) (s)	2135	2358.5	11,000	4220	7244	4320
Specific heat of evaporation, kJ/kg (h_{vl})	–	–	–	2257	2096	1070

Figure 2 shows the results of numerical computations for the case in which $p = 101.3$ kPa, produced using the Lee, Tanasawa, and Rohsenow models of boiling. The value of the coefficients of these models is varied in order to study the effect of their value on the position of the interface for this particular problem and method.



(**a**)

Figure 2. *Cont.*

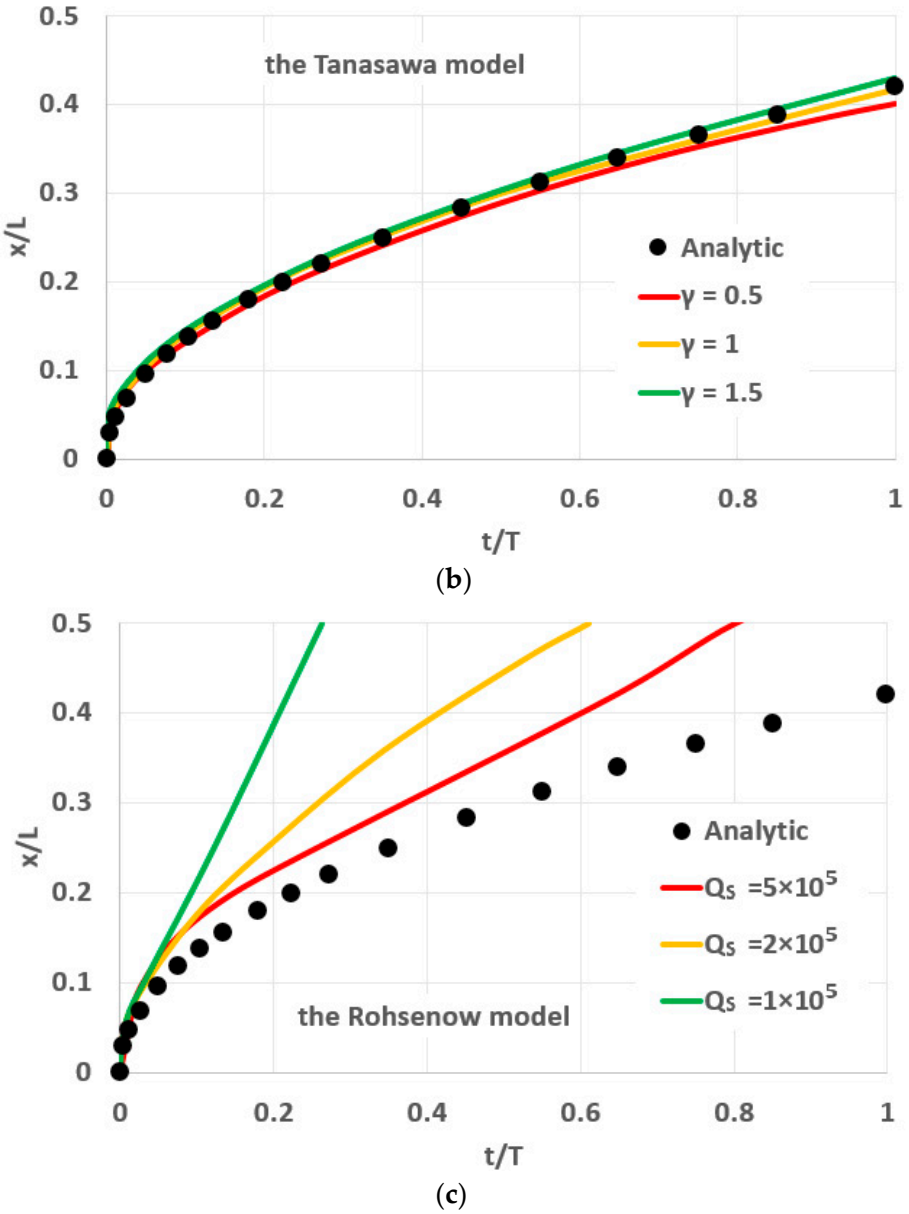
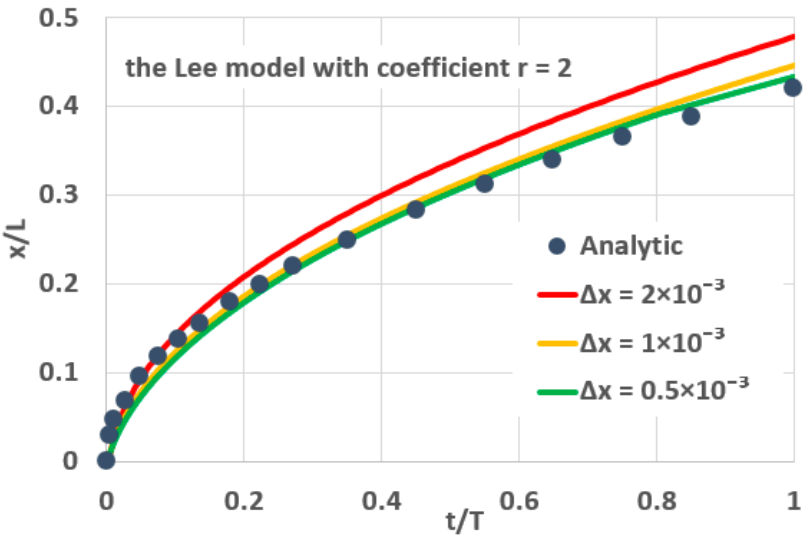


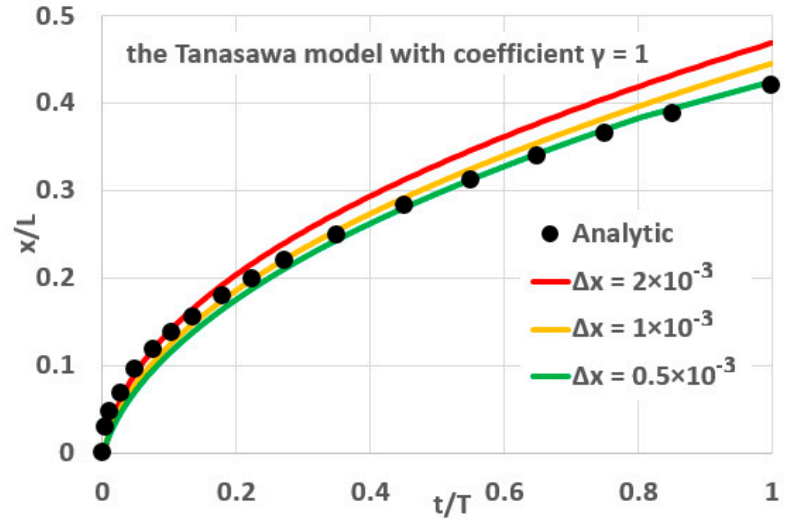
Figure 2. Interface position as a function of time at p = 101.3 kPa: (**a**) Lee model; (**b**) Tanasawa model; (**c**) Rohsenow model.

For the Lee model, at the value of $r = 1$, the plot of the interface position at the initial stage lies above the analytical solution. For values $3 < r < 10$, the plot has a better agreement with analytical data. In the Tanasawa model, in many publications [43,44], the value equal to 1 is taken as an optimal one of the γ parameter for the Stefan problem. $\gamma = 1$ is also set in the described computations. For the Rohsenow model, the result is noticeably worse, since the phase boundary moves faster than it should move according to calculations based on analytical formulas. It is not possible to achieve good agreement with the analytical data. At a heat transfer coefficient value of $Qs > 5 \times 10^5$, non-physical pressure surges appear and the calculation is completed as an emergency.

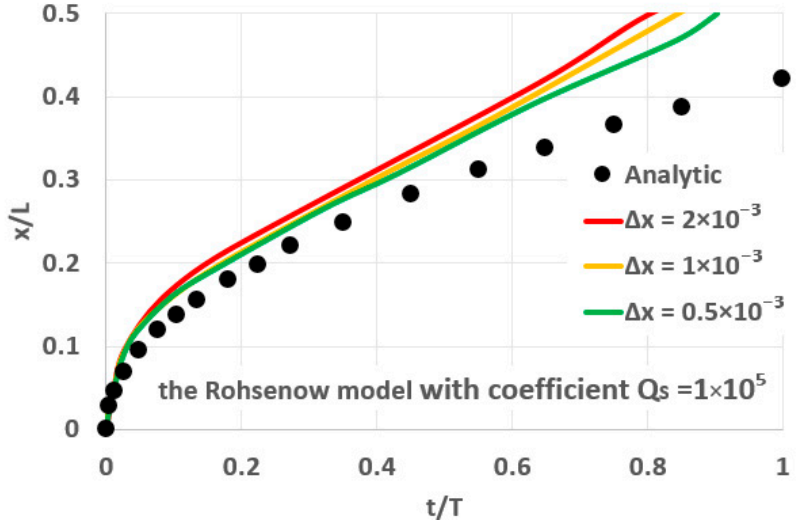
Figure 3 shows the plots of interface position versus time for meshes with characteristic cell size in the longitudinal direction of the channel produced using the Tanasawa model with a coefficient of $\gamma = 1$, the Lee model with a coefficient of $r = 2$ and the Rohsenow model with a coefficient of $Qs = 1 \times 10^5$.



(**a**)



(**b**)



(**c**)

Figure 3. Interface position as a function of time for meshes with characteristic sizes of cells $\Delta x = 0.5 \times 10^{-3}$, 1×10^{-3}, 2×10^{-3}: (**a**) the Lee model with coefficient $r = 2$; (**b**) the Tanasawa model with coefficient $\gamma = 1$; (**c**) the Rohsenow model with coefficient $Qs = 1 \times 10^5$.

The plots show the mesh convergence of the realized Tanasawa, Lee, and Rohsenow models. Figure 4 shows the plots of interface position versus time for computations using the Tanasawa, Lee, and Rohsenow models of boiling in comparison with analytics for all computed cases (Table 1). It follows from the figure that the Tanasawa model describes the analytics most accurately. The Lee model also produces acceptable results, especially for cases with p_{sat} = 571 kPa and 14,044 MPa. For these cases, the results of the Tanasawa and Lee models practically coincide. The Rohsenow model has the largest deviation from the reference data.

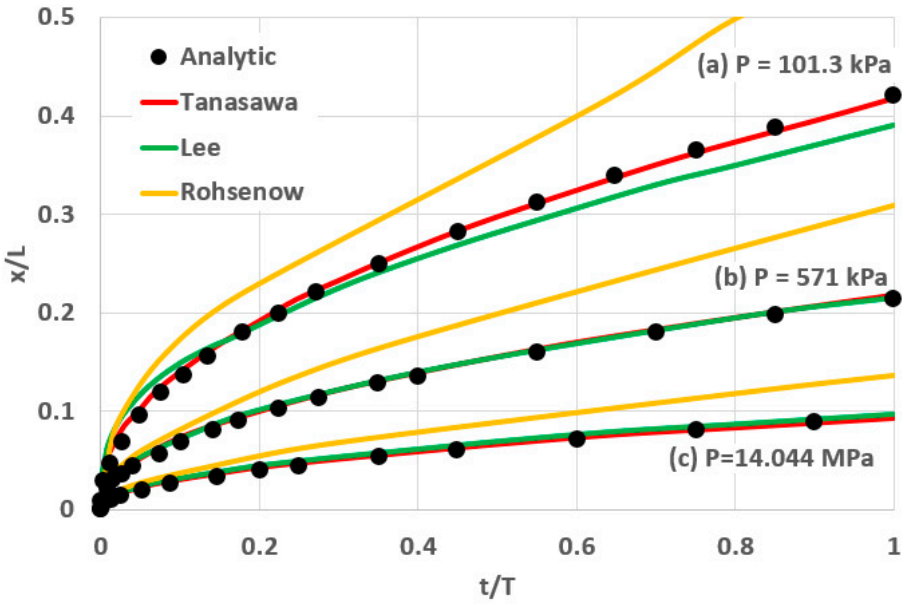


Figure 4. Comparison of the position of the interface obtained analytically and using the CFD model.

Figure 5 shows the interface for the time point $t = 0.025 \times T$ for computation using the Tanasawa model. It can be seen that the phase boundary is localized within two cells. There is no blurring of the phase boundary during its movement.

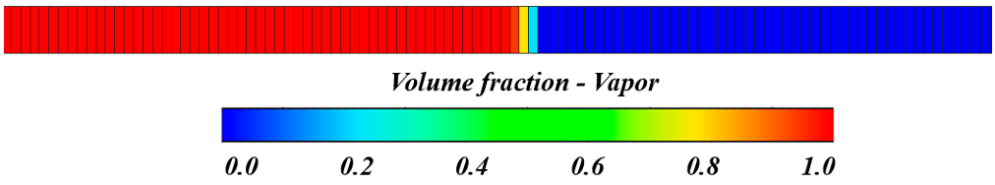


Figure 5. A typical distribution pattern for the volume fraction of vapor.

As a result of a series of numerical experiments, it is shown that the average computation error for the Lee model for computation cases (b) and (c) is up to 3%; for case I, it is 6%, and for the Tanasawa model, it is 1% and 3%, respectively. Moreover, the higher the pressure is, the smaller the computation error is. The results on Rohsenow model are slightly worse because the interface moves faster than it should according to the analytical model. The relative error increases with the movement of the phase boundary, and for the computation cases, (a) is 50% at the end of the calculation time t = T.

4.2. Single Vapor Bubble Condensation Problem

The floating up of a single bubble of saturated vapor in still water is simulated. At the initial time point, the vapor bubble with a diameter D = 1 mm is surrounded by water at a temperature 25 K less than the saturation temperature. Phase exchange at the phase

boundary leads to a decrease in the size of the bubble due to the condensation. Numerical simulation results are compared with the published experimental data [35,45].

Figure 6 shows the geometry of this problem.

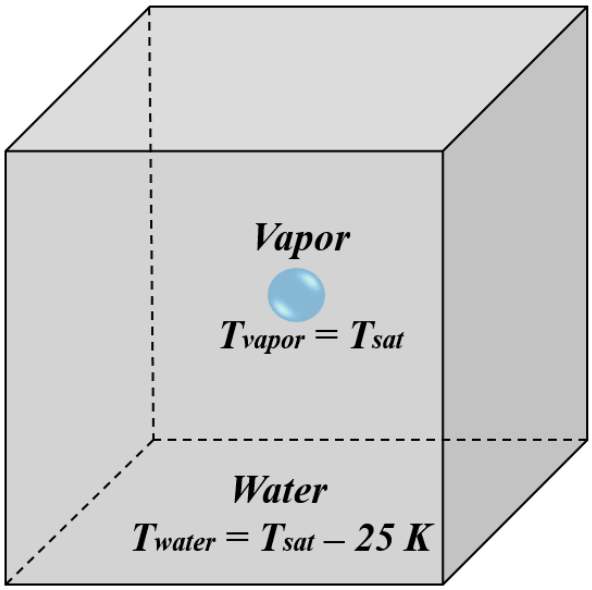


Figure 6. Geometry of the problem in the simulated region.

The problem is solved in a two-dimensional formulation on meshes that differ in characteristic cell size in the bubble area. Table 2 shows the parameters of the mesh models used.

Table 2. Parameters of mesh models.

Mesh	N°1	N°2	N°3
Relative size of cells, $\Delta x/D$	50	100	200
Number of cells	30,000	75,000	225,000

Figure 7 shows the ratio of bubble size and grid resolution for mesh N° 2.

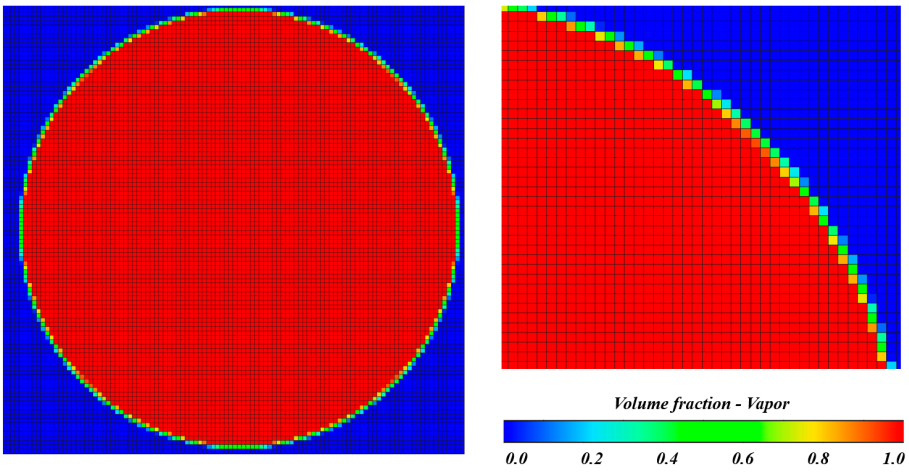


Figure 7. The ratio of bubble size and grid resolution for mesh N°2.

The following boundary conditions are used: a boundary condition of symmetry is set on the front and back surfaces of the modeling area, a fixed pressure is set on top, and a boundary condition of an impenetrable wall with slippage is set on all other boundary

surfaces. The temperature of the vapor at the initial time point is equal to the saturation temperature T_{sat} = 380.26 K at a pressure of 130 kPa, and the water temperature at the initial time point is equal to $T = (T_{sat} - 25)$ K. Table 3 shows the thermophysical properties of water and water vapor.

Table 3. Properties of water and water vapor for p_{sat} = 130 kPa.

	Vapor (ν)	**Liquid (*l*)**
Boiling (saturation) temperature, K (T_{sat})		380
Density, kg/m^3 (ρ)	0.75453	953.13
Dynamic viscosity, Pa × s (μ)	1.25×10^{-5}	2.6×10^{-4}
Thermal conductivity, W/(m × K) (k)	0.025905	0.68106
Specific heat at constant pressure, J/(kg × K) (Cp)	2110	4224
Specific heat of evaporation, kJ/kg (h_{vl})		2237
Surface tension, N/m (σ)		0.06

The following are the results of research on the effect of empirical coefficients on the accuracy of simulation for implemented methods on mesh No. 2. The changes in the shape and diameter of the bubble with time are compared with the experimental data.

Figure 8 shows the plots of the bubble diameter change with time produced in numerical computations using the Lee model with different values of parameter r.

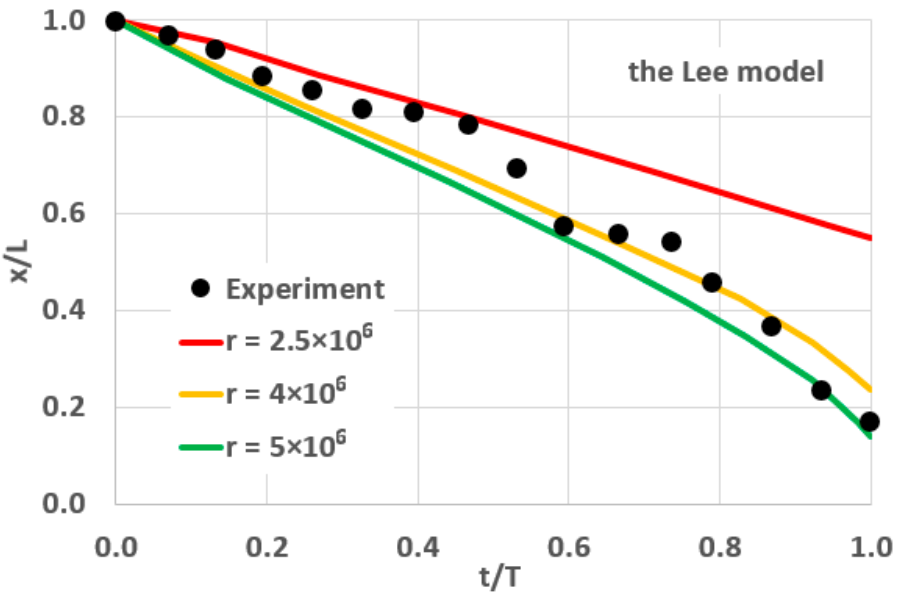


Figure 8. Changes in bubble diameter with time. Computations are carried out using the Lee model.

With the specified task parameters, a rather intensive mass exchange takes place. In such circumstances, a coefficient r of about 10^5~10^7 may be selected for the Lee model. When performing numerical computations, it is found out that the r = 4 × 10^6 coefficient is optimal for the presented procedure. At lower values of this coefficient, the results of numerical computations differ significantly from the experiment.

Figure 9 shows the results of numerical computations produced using the Tanasawa model of boiling for coefficient values of γ = 0.006, 0.007, and 0.01.

As it is said in [23,46,47], for experiments with single bubbles suspended in water to describe the boiling/condensation process in the Tanasawa model, the value of the empirical coefficient γ should be set at about 0.01. The coefficient γ = 0.006 is optimal for these simulation conditions. With the increase in γ, the results of numerical computations move further and further away from the experimental data. The result is quite sensitive to

the variation in coefficient γ. In the case of the Rohsenow model, the optimal value of the coefficient $Q_S = 1.7 \times 10^7$, as shown in Figure 10.

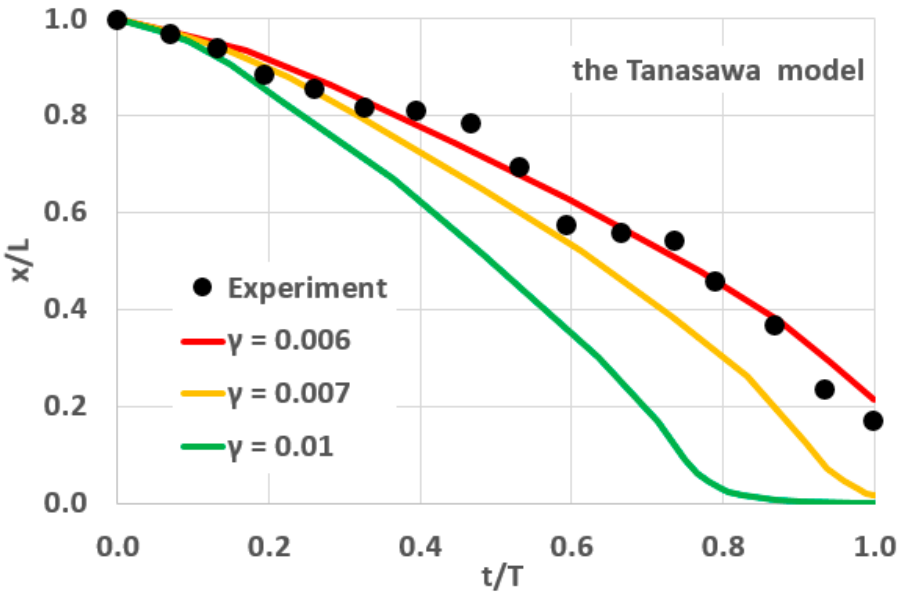


Figure 9. Changes in bubble diameter with time. Computations are carried out using the Tanasawa model.

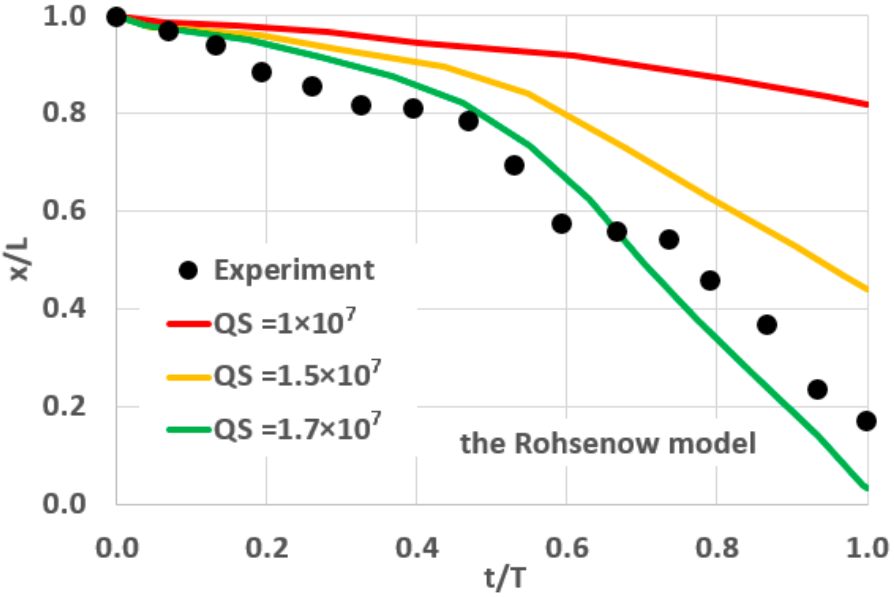


Figure 10. Changes in bubble diameter with time. Computations are carried out using the Rohsenow model.

Figure 11 shows the results of the computations for all three models under study with the optimal values of empirical parameters determined earlier. It follows from the plots that all three models describe the experiment well.

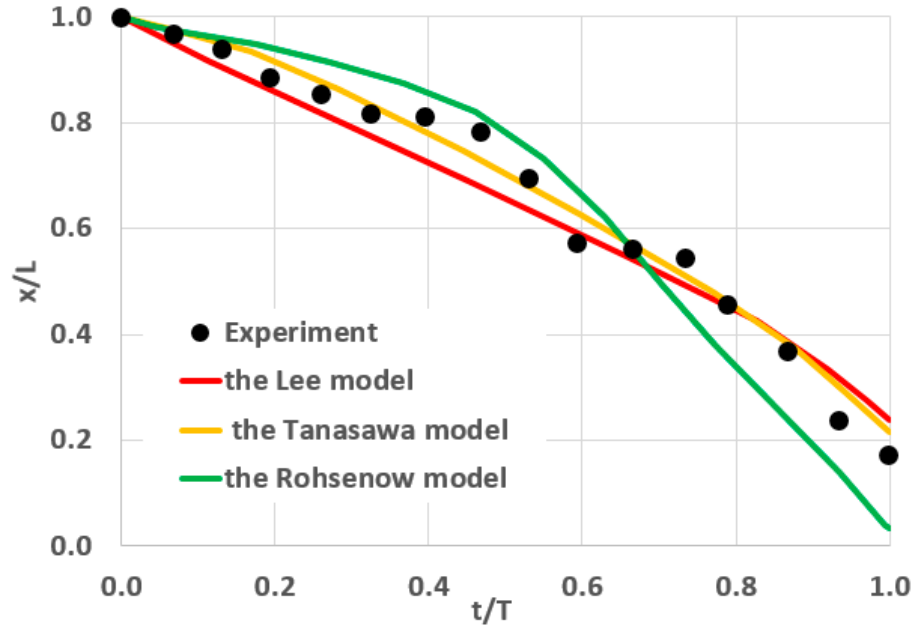
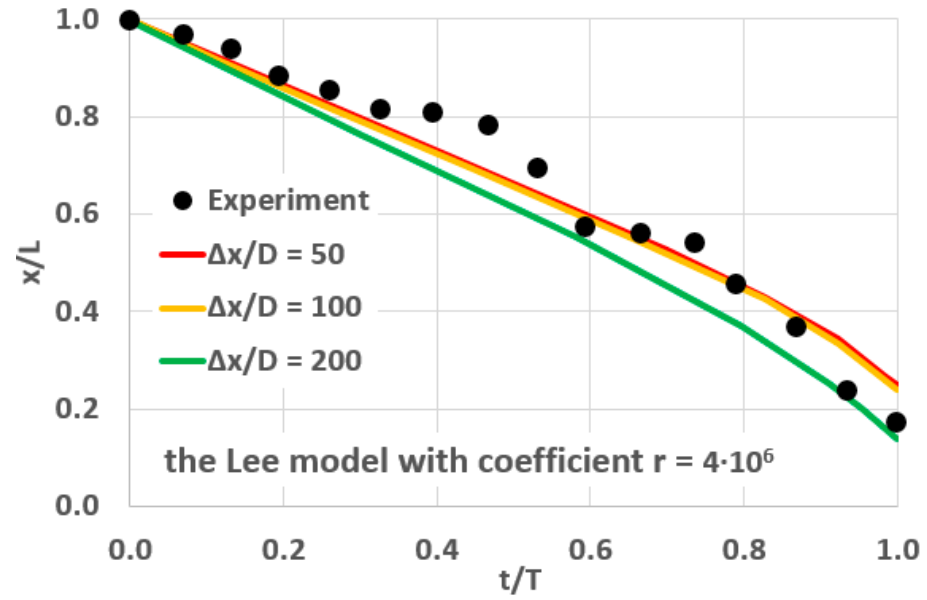


Figure 11. Changes in bubble diameter with time.

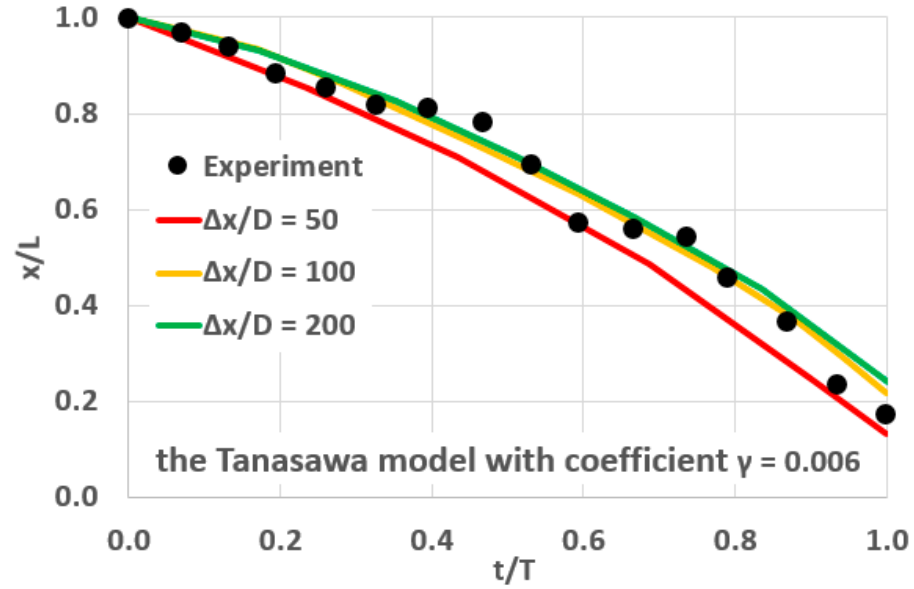
Figure 12 shows plots of the changes in bubble diameter with time for meshes with relative cell sizes of Δx/D = 50, 100, and 200 for the Lee model with coefficient $r = 4 \times 10^6$, the Tanasawa model with coefficient γ = 0.006, and the Rohsenow model with coefficient $Qs = 1.7 \times 10^7$.

Graph analysis shows that all implemented phase change models have the property of grid convergence. It is shown that grid model No. 2 with a relative cell size of Δx/D = 100 is the best choice for calculations. Calculations on the specified grid have sufficient accuracy; in addition, they take less time to carry out calculations than calculations on a grid with a smaller characteristic cell size.

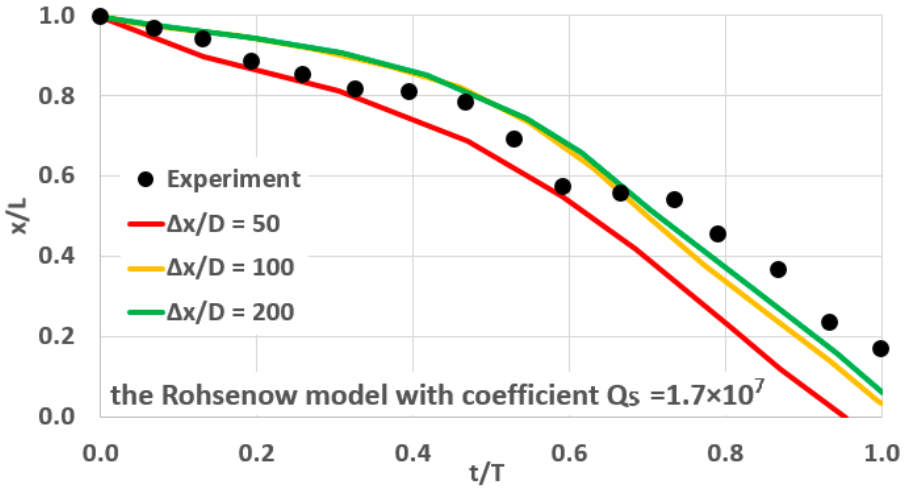


(**a**)

Figure 12. *Cont.*



(**b**)



(**c**)

Figure 12. Changes in bubble diameter with time for meshes with relative cell sizes of Δx/D = 50, 100, and 200: (**a**) the Lee model with coefficient $r = 4 \times 10^6$; (**b**) the Tanasawa model with coefficient $\gamma = 0.006$; (**c**) the Rohsenow model with coefficient $Qs = 1.7 \times 10^7$.

Analyzing the obtained calculated data, we can conclude that of the three implemented phase change models, the Tanasawa model is closest to the experimental values of the diameter of the condensed bubble. Figure 13 shows the dynamics of the change in the shape of the bubble over time, with comparison of numerical calculations using the Tanasawa model carried out in this article, numerical calculations using OpenFOAM [48], and experimental photographs of the shape of the bubble [49]. There is good agreement between the experimental data and the computations.

We can conclude, based on the results of the problem of vapor bubble condensation, that all implemented methods allow problems of this class to be solved. The Tanasawa model has the greatest accuracy; the Rohsenow model is most unstable and prone to deformations of the bubble shape.

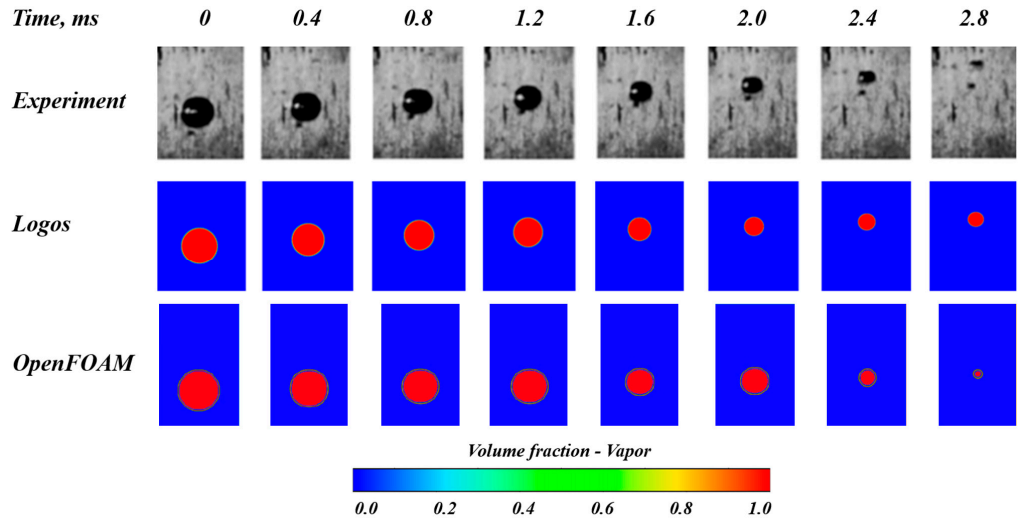


Figure 13. Changes in bubble diameter: experimental values (upper row), numerical studies conducted in this article (middle row), and numerical studies conducted in OpenFOAM [48] (bottom row).

5. Conclusions

This paper presents the results of a study of the possibility of using a single-speed multiphase liquid model with free surface allowance for simulating boiling and condensation processes. To account for the phase interface, the VOF method is used and is implemented on the basis of finite volume sampling on unstructured grids. A modification of the basic mathematical model, namely the volume fraction transfer equations, is made, which helps to increase the stability of the iterative procedure for numerically solving problems on arbitrary unstructured grids. The models of Tanasawa, Lee, and Rohsenow are considered models of interphase mass transfer in which the evaporated or condensed mass linearly depends on the difference between local temperature and saturation temperature with accuracy in empirical parameters. Empirical parameters are calibrated for these mass transfer models. The research herein is carried out using the classical Stefan problem of the movement of the interphase boundary due to the evaporation of liquid and the problem of condensation of a vapor bubble in a water column. It is shown that the average error in the position of the interfacial boundary in the Stefan problem for the Tanasawa and Lee models does not exceed 3–6%, while the corresponding result is slightly worse for the Rohsenow model. In the problem of a floating condensing vapor bubble, it is shown that the Tanasawa model has the highest accuracy, while the Rohsenow model is most unstable and prone to deformation of the bubble shape. At the same time, the dynamics of bubble ascent are modeled correctly by all three models.

The results of the solution of these problems confirm the fundamental possibility of using a VOF method for simulating boiling and condensation processes, taking into account the dynamics of the free surface. However, they reveal the problem of the phase transition models under consideration: the optimal value of empirical parameters should be selected for each task and formulation depending on the conditions of the problem, the parameters of the computational model, and the characteristic size of the grid model cells.

Author Contributions: Conceptualization, A.K. (Andrey Kozelkov) and A.K. (Andrey Kurkin); data curation, V.K., A.P., N.T. and V.G.; formal analysis, A.K. (Andrey Kozelkov) and V.K.; investigation, A.K. (Andrey Kozelkov), A.K. (Andrey Kurkin), V.K., A.P., N.T. and V.G.; methodology, A.K. (Andrey Kozelkov) and A.K. (Andrey Kurkin); software, A.P., N.T. and V.G.; supervision, A.K. (Andrey Kurkin); validation, A.P., N.T. and V.G.; visualization, V.K. and V.G.; writing—original draft, A.K. (Andrey Kozelkov) and A.K. (Andrey Kurkin); writing—review and editing, A.K. (Andrey Kozelkov)

and A.K. (Andrey Kurkin). All authors have read and agreed to the published version of the manuscript.

Funding: This research was funded by the Ministry of Science and Higher Education of the Russian Federation (project No. FSWE-2024-0001 (research topic: "Developing numerical methods, models and algorithms to describe liquid and gas flows in natural environment, and in the context of industrial objects' operation in standard and emergency conditions on mainframes with exa- and zeta capacity")).

Data Availability Statement: The original contributions presented in this study are included in the article. Further inquiries can be directed to the corresponding author.

Conflicts of Interest: The authors declare no conflicts of interest.

References

1. Ferrín, J.L.; Pérez-Pérez, L.J. Numerical simulation of natural convection and boil-off in a small size pressurized LNG storage tank. *Comput. Chem. Eng.* **2020**, *138*, 106840. [CrossRef]
2. Roh, S.; Son, G. Numerical study of natural convection in a liquefied natural gas tank. *J. Mech. Sci. Technol.* **2012**, *26*, 3133–3140. [CrossRef]
3. Tyatyushkina, E.S.; Kozelkov, A.S.; Kurkin, A.A.; Kurulin, V.V.; Efremov, V.R.; Utkin, D.A. Evaluation of numerical diffusion of the finite volume method when modelling surface waves. *Comput. Technol.* **2019**, *24*, 106–119. [CrossRef]
4. Kozelkov, A.; Kurulin, V.; Kurkin, A.; Taranov, A.; Plygunova, K.; Krutyakova, O.; Korotkov, A. Numerical Approach Based on Solving 3D Navier–Stokes Equations for Simulation of the Marine Propeller Flow Problems. *Fluids* **2023**, *8*, 293. [CrossRef]
5. Korotkov, A.V.; Kozelkov, A.S.; Kurkin, A.A.; Giniyatullin, R.R.; Lashkin, S.V. Numerical Simulation of the Conjugate Heat Transfer of a «Fluid–Solid Body» System on an Unmatched Grid Interface. *Fluids* **2023**, *8*, 266. [CrossRef]
6. Kurul, N.; Podowski, M. Multidimensional effects in forced convection subcooled boiling. In Proceedings of the Ninth International Heat Transfer Conference, Jerusalem, Israel, 19–24 August 1990.
7. Yang, K.; Hong, F.; Cheng, P. A fully coupled numerical simulation of sessile droplet evaporation using Arbitrary Lagrangian-Eulerian formulation. *Int. J. Heat Mass Transf.* **2014**, *70*, 409–420. [CrossRef]
8. Wang, H.; Pan, Z.; Garimella, S.V. Numerical investigation of heat and mass transfer from an evaporating meniscus in a heated open groove. *Int. J. Heat Mass Transf.* **2011**, *54*, 3015–3023. [CrossRef]
9. Hirt, C.W.; Nichols, B. Volume of fluid (VOF) method for dynamics of free boundaries. *J. Comput. Phys.* **1981**, *39*, 201–225. [CrossRef]
10. Osher, S.; Sethian, J.A. Fronts propagating with curvature-dependent speed: Algorithms based on Hamilton-Jacobi formulations. *J. Comput. Phys.* **1988**, *79*, 12–49. [CrossRef]
11. Cerne, G.; Petelinb, S.; Tiselja, I. Coupling of the Interface Tracking and the Two-Fluid Models for the Simulation of Incompressible Two-Phase Flow. *J. Comput. Phys.* **2001**, *171*, 776–804. [CrossRef]
12. Li, L.; Niu, Y.; Wei, G.; Manickam, S.; Sun, X.; Zhu, Z. Investigation of cavitation noise using Eulerian-Lagrangian multiscale modeling. *Ultrason. Sonochem.* **2023**, *97*, 106446. [CrossRef]
13. Alkhezzi, A.; Fan, Y. Improved Two-Fluid Model for Segregated Flow and Integrated Multiphase Flow Modeling for Downhole Pressure Predictions. *Energies* **2023**, *16*, 7923. [CrossRef]
14. Zürner, T.; Kamble, V.; Rzehak, R.; Eckert, K. Experimental and numerical investigation of turbulent multiphase jets. *Miner. Eng.* **2024**, *211*, 108699. [CrossRef]
15. Meng, L.; Gao, S.; Wei, D.; Zhao, Q.; Cui, B.; Shen, Y.; Song, Z. Particulate flow modelling in a spiral separator by using the Eulerian multi-fluid VOF approach. *Int. J. Min. Sci. Technol.* **2023**, *33*, 251–263. [CrossRef]
16. Ubbink, O. Numerical Prediction of Two Fluid Systems with Sharp Interfaces. Ph.D. Thesis, University of London, London, UK, 1997.
17. Kozelkov, A.S.; Pogosyan, M.A.; Strelets, D.Y.; Tarasova, N.V. Application of mathematical modeling to solve the emergency water landing task in the interests of passenger aircraft certification. *Aerosp. Syst.* **2021**, *4*, 75–89. [CrossRef]
18. Kozelkov, A.S.; Kurkin, A.A.; Kurulin, V.V.; Lashkin, S.V.; Tarasova, N.V.; Tyatyushkina, E.S. Numerical Modeling of the Free Rise of an Air Bubble. *Fluid Dyn.* **2016**, *51*, 709–721. [CrossRef]
19. Kozelkov, A.; Galanov, N.; Semenov, I.; Zhuchkov, R.; Strelets, D. Computational Investigation of the Water Droplet Effects on Shapes of Ice on Airfoils. *Aerospace* **2023**, *10*, 906. [CrossRef]

20. Knudsen, M. *The Kinetic Theory of Gases. Some Modern Aspects*; Methuen and Co., Ltd.: London, UK, 1934.
21. Schrage, R.W. *A Theoretical Study of Interphase Mass Transfer*; Columbia University Press: New York, NY, USA, 1953.
22. Kharangate, C.R.; Mudawar, I. Review of computational studies on boiling and condensation. *Int. J. Heat Mass Transf.* **2017**, *108*, 1164–1196. [CrossRef]
23. Tanasawa, I. Advances in condensation heat transfer. In *Advances in Heat Transfer*; Hartnett, J.P., Irvine, T.F., Eds.; Academic Press: San Diego, CA, USA, 1991; Volume 21.
24. Lee, W.H. A Pressure Iteration Scheme for Two-Phase Flow Modeling. In *Multiphase Transport Fundamentals, Reactor Safety, Applications*; Hemisphere: Washington, DC, USA, 1980.
25. Rohsenow, W.M. A method of correlating heat transfer data for surface boiling of liquids. *Trans. ASME* **1952**, *74*, 969–976. [CrossRef]
26. Sharif, S.A.; Ho, M.K.M.; Timchenko, V.; Yeoh, G.H. Numerical study of effects of system variables on rising vapour bubble in convective boiling conditions. *Ann. Nucl. Energy* **2025**, *222*, 111553. [CrossRef]
27. Darshan, M.B.; Magnini, M.; Matar, O.K. Numerical simulations of flow boiling in constricted microchannels: Bubble dynamics and heat transfer characteristics. *Int. J. Heat Mass Transf.* **2025**, *253*, 127456. [CrossRef]
28. Vishal; Rohilla, L.; Kumar, P. Numerical investigation of drop spreading on a heated surface. *Sustain. Chem. Clim. Action* **2025**, *6*, 100065. [CrossRef]
29. Li, Q.; Ge, H.; Pan, R.; Zhang, Z.; Chen, R. Numerical Study on Flow and Release Characteristics of Gas Extinguishing Agent under Different Filling Pressure and Amount Conditions. *Processes* **2021**, *9*, 1683. [CrossRef]
30. Wan, H.; Hu, J.; Gao, L.; Miao, X.; Xu, Y. Unsteady numerical calculation of flow boiling heat transfer in microchannels with Kagome structures. *Case Stud. Therm. Eng.* **2024**, *63*, 105289. [CrossRef]
31. Caner, J.; Videcoq, E.; Benselama, A.M.; Girault, M. Simulation of a two-phase loop thermosyphon using a new interface-resolved phase change model. *Int. J. Heat Mass Transf.* **2024**, *228*, 125607. [CrossRef]
32. Liu, S.; Chen, J.; Ji, W.; Tong, Z.; Fu, Y.; Qian, N.; Dai, C. Analysis of pool boiling heat transfer characteristics on copperbased structured surfaces modified with superhydrophilic, hydrophobic, superhydrophobic and hybrid biphilic properties. *Case Stud. Therm. Eng.* **2024**, *61*, 105044. [CrossRef]
33. Brackbill, J.U.; Kothe, D.B.; Zemach, C. A continuum method for modeling surface tension. *J. Comput. Phys.* **1992**, *100*, 335–354. [CrossRef]
34. Welch, S.W.; Wilson, J. A volume of fluid based method for fluid flows with phase change. *J. Comput. Phys.* **2000**, *160*, 662–682. [CrossRef]
35. Kamei, S.; Hirata, M. Condensing phenomena of a single vapor bubble into subcooled water. *Exp. Heat Transf. Int. J.* **1990**, *3*, 173–182. [CrossRef]
36. Ferziger, J.H.; Peric, M. *Computational Method for Fluid Dynamics*; Springer: New York, NY, USA, 2002.
37. Vachaparambil, K.J.; Einarsrud, K.E. Comparison of Surface Tension Models for the Volume of Fluid Method. *Processes* **2019**, *7*, 542. [CrossRef]
38. Lee, H.; Kharangate, C.R.; Mascarenhas, N.; Park, I.; Mudawar, I. Experimental and computational investigation of vertical downflow condensation. *Int. J. Heat Mass Transf.* **2015**, *85*, 865–879. [CrossRef]
39. Efremov, V.R.; Kozelkov, A.S.; Kornev, A.V.; Kurkin, A.A.; Kurulin, V.V.; Strelets, D.Y.; Tarasova, N.V. Method for taking into account gravity in free-surface flow simulation. *Comput. Math. Math. Phys.* **2017**, *57*, 1720–1733. [CrossRef]
40. Landau, L.D.; Lifshitz, V.M. *Hydrodynamics*; Nauka: Moscow, Russia, 1988.
41. Lashkin, S.V.; Kozelkov, A.S.; Yalozo, A.V.; Gerasimov, V.Y.; Zelensky, D.K. Efficiency Analysis of the Parallel Implementation of the SIMPLE Algorithm on Multiprocessor Computers. *J. Appl. Mech. Tech. Phys.* **2017**, *58*, 1242–1259. [CrossRef]
42. Sarazov, A.V.; Kozelkov, A.S.; Strelets, D.Y.; Zhuchkov, R.N. Modeling Object Motion on Arbitrary Unstructured Grids Using an Invariant Principle of Computational Domain Topology: Key Features. *Symmetry* **2023**, *15*, 2081. [CrossRef]
43. Giustini, G.; Issa, R.I. A method for simulating interfacial mass transfer on arbitrary meshes. *Phys. Fluids* **2021**, *33*, 087102. [CrossRef]
44. Magnini, M.; Pulvirenti, B.; Thome, J.R. Numerical investigation of hydrodynamics and heat transfer of elongated bubbles during flow boiling in a microchannel. *Int. J. Heat Mass Transf.* **2013**, *59*, 451–471. [CrossRef]
45. Kamei, S.; Hirata, M. Study on condensation of a single vapor bubble into subcooled water—Part 2; Experimental analysis. *Heat Trans.–Jpn. Res.* **1990**, *19*, 1–10.
46. Hardt, S.; Wondra, F. Evaporation model for interfacial flows based on a continuum-field representation of the source terms. *J. Comput. Phys.* **2008**, *227*, 5871–5895. [CrossRef]
47. Marek, R.; Straub, J. Analysis of the evaporation coefficient and the condensation coefficient of water. *Int. J. Heat Mass Transf.* **2001**, *44*, 39–53. [CrossRef]

48. Zeng, Q.; Cai, J.; Yin, H. Numerical simulation of single bubble condensation in subcooled flow using OpenFOAM. *Prog. Nucl. Energy* **2015**, *83*, 336–346. [CrossRef]
49. Samkhaniani, N.; Ansari, M. Numerical simulation of bubble condensation using CF-VOF. *Prog. Nucl. Energy* **2016**, *89*, 120–131. [CrossRef]

Disclaimer/Publisher's Note: The statements, opinions and data contained in all publications are solely those of the individual author(s) and contributor(s) and not of MDPI and/or the editor(s). MDPI and/or the editor(s) disclaim responsibility for any injury to people or property resulting from any ideas, methods, instructions or products referred to in the content.